Diatomic Silylynes, Germylynes, Stannylynes, and Plumbylynes: Structures, Dipole Moments, Dissociation Energies, and Quartet-Doublet Gaps of EH and EX (E = Si, Ge, Sn, Pb; X = F, Cl, Br, I)

Huidong Li,[†,‡] Hao Feng,[*,†,‡] Weiguo Sun,[†,‡] Yaoming Xie,[§] and Henry F. Schaefer[*,§]

[†]School of Physics and Chemistry, Research Center for Advanced Computation, Xihua University, Chengdu, China 610039

[‡]Institute of Atomic and Molecular Physics, Sichuan University, Chengdu, Sichuan 610065, China

[§]Department of Chemistry and Center for Computational Chemistry, University of Georgia, Athens, Georgia 30602, United States

ABSTRACT: Systematic theoretical studies of the carbyne and halocarbyne analogues E-H and E-X (E = Si, Ge, Sn, Pb; X = F, Cl, Br, I) were carried out with ab initio coupled-cluster methods using very large basis sets. The $^2\Pi$ state is the ground electronic state for all these compounds. The quartet-doublet energy separations, equilibrium distances, and dissociation energies for these species are predicted. The quartet-doublet splittings fall in the order EF > ECl > EBr > EI > EH for a given metal E; and PbX > GeX > SnX > SiX for the same halogen atom X. The dipole moments span a large range, from 0.08 debye (GeH) to 3.58 debye (PbCl). The dissociation energies range from 1.84 eV (PbH) to 6.15 eV (SiF).
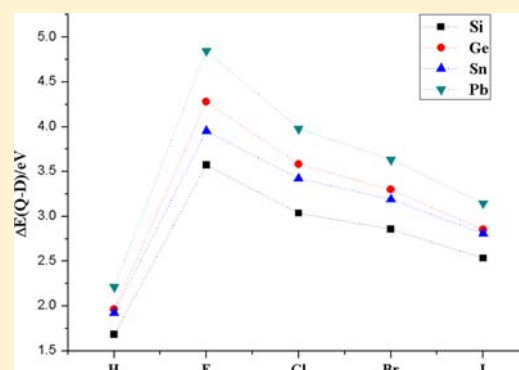
INTRODUCTION

One of the inspiring attractions of chemistry is the way in which nonexistent molecules are finally detected and how "transient" species become "stable".[1] Monovalent carbon compounds provide a simple example of this procession of molecules from unknown to important. The carbynes CR have gone from exotic fleeting species to play a significant role in combustion chemistry.[2−6] The analogous coming-of-age for monovalent silicon, germanium, tin, and lead compounds is captured in the title of the recent book by Lee and Sekiguchi.[7] Important recent synthetic studies include the synthetic work of Hashimoto et al.[8] and by Filippou and co-workers on organometallic silylynes and germylynes.[9−13]

Compared with the carbynes, the analogous species E-H and E-X (E = Si, Ge, Sn, Pb; X = F, Cl, Br, I) have been less studied. The optical spectrum for the SiH radical was first reported in 1930.[14] The $^2\Pi$ ground state of SiH has now been studied by laser photoelectron spectrometry, laser-induced fluorescence, the vibration−rotation spectrum, and optical emission spectroscopy.[15−18] A series of theoretical studies on SiH was summarized by Kalemos and Mavridis in 2002.[19]

The halosilylynes, SiX (X = F, Cl, Br, I), have been detected as $^2\Pi$ ground states by spectroscopic methods, motivated by their importance in understanding silicon chemical vapor deposition (CVD) processes.[20,21] The theoretical work of Lein, Krapp, and Frenking[22] on SiH, GeH, SnH, and PbH is especially noteworthy. Theoretical studies of the silicon halides have also reported.[23−28] The halogermylynes have been studied to assess their roles in processing semiconductors.[29−34]

Stannylynes have proved to be important in understanding new organometallic chemistry.[35] However, isolated low-valence stannylynes R-Sn(I) are rarely observed since usually they are assumed to be unstable species. Practically speaking, R-Sn radicals are usually intermediates in transformations to the stable Sn(IV) or Sn(II) compounds.[36]

For the lead monofluoride molecule PbF, planned experiments to search for the simultaneous violation of time-reversal (T) and space parity (P) invariance have motivated special theoretical interest.[37−39] The lead halides PbH, PbF, PbCl, PbBr, and PbI have been studied in an important paper by Shimizu and Frenking.[40]

In recent years, Fillippou and co-workers have reported the syntheses of metal-silylyne and metal-germylyne complexes containing E-X ligands.[9−12] When these silylynes and germylynes are coordinated to a transition-metal center, their reactivity is altered profoundly. Thus the mononuclear halosilylyne complexes are promising precursors for new compounds with metal−silicon and metal−germanium multiple bonds.[9]

Theoretical studies for transition metal complexes containing the M-E-Me bonds (M = Cr, Mo, W; E = Si, Ge, Sn, Pb) have also been reported.[41] However, systematical theoretical studies on the isolated E-H and E-X (E = Si, Ge, Sn, Pb, X = F, Cl, Br, I) species are scarce. The present work will systematically investigate these diatomic molecules, with emphasis on their

geometries, dipole moments, electronic structures, quartet-doublet splitting, and dissociation energies.

2. THEORETICAL APPROACH

All geometries are optimized with single and double excitation coupled-cluster theory with perturbative triples CCSD(T).[42−44] The optimizations were performed with the CFOUR program.[45] For H, F, Cl, and Si atoms, the correlation-consistent cc-pVnZ and cc-pwCVnZ (n = T, Q, 5) basis sets[46−48] are used. For the Ge, Sn, Pb, Br, and I atoms, the Stuttgart-Cologne MCDHF (multiconfiguration Dirac−Hartree−Fock adjusted) effective core potentials (ECP) and the corresponding correlation-consistent cc-pVnZ-PP and cc-pwCVnZ-PP (n = T, Q, 5) basis sets were utilized.[49−53] With these ECPs, 10 core electrons ($1s^2 2s^2 2p^6$) are embodied in the effective cores for Ge and Br, 28 core electrons ($1s^2 2s^2 2p^6 3s^2 3p^6 3d^{10}$) for Sn and I, and 60 core electrons ($1s^2 2s^2 2p^6 3s^2 3p^6 3d^{10} 4s^2 4p^6 4d^{10} 4f^{14}$) for Pb. With the coupled-cluster methods used in this research, the core orbitals are frozen. That is, the 1s orbital is frozen for F, while the 1s2s2p orbitals are frozen for Si and Cl. Since the d^{10} electrons are important for the Ge($3d^{10}$), Br($3d^{10}$), Sn($4d^{10}$), I($4d^{10}$), and Pb($5d^{10}$) atoms, only up to the 3s3p orbitals are frozen for Ge and Br, with up to 4s4p orbitals frozen for Sn and I, and up to 5s5p for Pb. In the present paper, we will use the more general notations cc-pVnZ(-PP) and cc-pwCVnZ(-PP) to represent both the all-electron cc-pVnZ and cc-pwCVnZ basis sets (for Si, F, and Cl) and the pseudopotential cc-pVnZ-PP and cc-pwCVnZ-PP basis sets (for Ge, Sn, Pb; Br, and I).

The correlation energy was also extrapolated to the complete basis set (CBS) limit by using the results from the cc-pwCVnZ(-PP) (n = Q, 5) basis sets via the following equations.[54]

$$E_{\text{total}} = E_{\text{HF}} + \Delta E_{\text{CCSD(T)}}^{\infty}$$

$$\Delta E_{\text{CCSD(T)}}^{n} = \Delta E_{\text{CCSD(T)}}^{\infty} - \frac{a}{n^3}$$

The minima on the potential energy surfaces at the cc-pwCVnZ(-PP) (n = Q, 5) and the CBS levels were obtained by fitting the total energies of seven points with a spacing of 0.03 Å around the equilibrium bond length with polynomial functions up to sixth order.
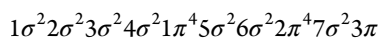
3. RESULTS AND DISCUSSION

The E-X (E = Si, Ge, Sn, Pb; X = F, Cl, Br, I) diatomics are readily seen to have low-lying doublet ($^2\Pi$) or quartet ($^4\Sigma^-$) electronic states (Scheme 1).
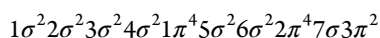
Scheme 1. Doublet ($^2\Pi$) and Quartet ($^4\Sigma^-$) States for the E-X (E = Si, Ge, Sn, Pb; X = F, Cl, Br, I) Compounds
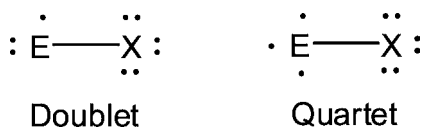
To use SiF, as an example, the doublet ($^2\Pi$) ground state has the electronic configuration

$$1\sigma^2 2\sigma^2 3\sigma^2 4\sigma^2 1\pi^4 5\sigma^2 6\sigma^2 2\pi^4 7\sigma^2 3\pi$$

and the lowest energy quartet ($^4\Sigma^-$) state has the electronic configuration,

$$1\sigma^2 2\sigma^2 3\sigma^2 4\sigma^2 1\pi^4 5\sigma^2 6\sigma^2 2\pi^4 7\sigma 3\pi^2$$

For other E-X compounds, the electronic configurations are analogous to those for SiF. In the present research we study both the $^2\Pi$ and $^4\Sigma^-$ states, and derive the quartet-doublet splittings from the high level CCSD(T) method with cc-pVnZ(-PP) basis sets (n = T, Q, 5) and cc-pwCVnZ(-PP) (n = Q, 5), then extrapolate to the complete basis sets(CBS). The

bond distances and dissociation energies are also studied, and our theoretical results will be compared with available experiments. We will mainly discuss the more reliable CCSD(T)/cc-pwCV5Z(-PP) results and the CBS results.

3.1. Quartet-Doublet Splittings. The doublet ($^2\Pi$) energies for the E-H and E-X compounds (E = Si, Ge, Sn, Pb; X = F, Cl, Br, I) are all predicted to be lower than the corresponding quartet ($^4\Sigma^-$) energies. The total energies and the quartet-doublet splittings ΔE(Q-D) at different levels of theory are shown in Table 1 and Figure 1.

An experimental ΔE(Q-D) value has been reported for SiH to be 5000 cm^{-1} (= 0.620 eV),[55] much smaller than our prediction of 1.683 eV (CCSD(T)/cc-pwCV5Z) or 1.688 eV (CBS). In fact, this experimental result was earlier shown to be unreliable by Kalemos and Mavridis.[19] Mavridis gave the theoretical ΔE(Q-D) results 35.53 (CASSCF), 38.77 (MRCI), 38.90 (MRCI+Q), and 38.89 (CCSD(T)) kcal/mol. The latter is very close to our result 1.683 eV (= 38.74 kcal/mol) or 1.688 eV (= 38.93 kcal/mol). For GeF, one must note the important experimental paper of Martin and Merer.[34] The experimental doublet-quartet splitting from the $^2\Pi_{1/2}$ ground state to the $^4\Sigma^-$ state of GeF was reported to be 4.32 eV,[34] which is comparable with our theoretical value of 4.28 or 4.30 eV (Table 1). The spin−orbital coupling (SOC) effect for the quartet-doublet splitting is not significant, and we will discuss it in section 3.5.

For the hydrides, that is, SiH, GeH, SnH, and PbH, the ΔE(Q-D) values are significantly smaller than those for the corresponding halides, SiX, GeX, SnX, and PbX (X = F, Cl, Br, I). As an example, for SiH and SiF, the Q-D splitting for SiH is ∼2 eV smaller than that for SiF (Figure 1 and Table 1). This difference may be explained partly via the orbital energies. Figure 2 shows that the quartet ($a^4\Sigma^-$) SiH has the $5\sigma 2\pi^2$ occupancy, which requires the one-electron promotion $5\sigma \rightarrow 2\pi$ from the $5\sigma^2 2\pi$ occupancy for doublet ($X^2\Pi$) SiH. Similarly, from the doublet SiF ($X^2\Pi$) to the quartet SiF ($a^4\Sigma^-$), one electron is excited from 7σ to 3π. Since the orbital-energy difference between 5σ to 2π in SiH is 2.5 eV, and that between 7σ to 3π in SiF is much larger (5.4 eV, Figure 2), the ΔE(Q-D) values are reflected.

Among the halides, the fluorides have the largest ΔE(Q-D) quartet-doublet splittings, while the iodides have the smallest, with the order E-F > E-Cl > E-Br > E-I (Figure 1 and Table 1). For example, the ΔE(Q-D) values for SiF, SiCl, SiBr, and SiI are predicted to be 3.57, 3.04, 2.86, and 2.54 eV, respectively, at the CCSD(T)/cc-pwCV5Z(-PP) level of theory, or 3.58, 3.05, 2.87, and 2.55 eV respectively, at the CBS level (Table 1). This trend is also consistent with the orbital-energy differences between the highest occupied σ and π orbitals, which are predicted to be 5.35, 4.00, 3.42, and 2.61 eV, respectively, for SiF, SiCl, SiBr, and SiI at the ROHF/cc-pwCV5Z(-PP) level. The same trend was also observed in a recent MRCI-SD(Q) study of ΔE(Q-D) for PbX by Frenking et al.[40]

Comparing the ΔE(Q-D) values for the same halogen (F, Cl, Br, I) atoms but different metals (Si, Ge, Sn, Pb), we find that they do not increase monotonically from Si to Pb, but are in the order PbX > GeX > SnX > SiX. In contrast to the periodic table positions of Ge and Sn, the ΔE(Q-D) value for each GeX is slightly larger than the corresponding value for SnX. This trend is reflected in the orbital energy differences of the highest occupied π and σ orbitals, similar to the discussion for the halides in the previous paragraph. For example, the orbital energy differences between the highest occupied σ and π orbitals are 3.42, 3.52, 3.47, and 3.66 eV for SiBr, GeBr, SnBr,

Table 1. Total Energies (*E*, in hartree) with Different Levels of Theory, and Quartet-Doublet Splittings Δ*E*(Q-D) (in eV) Predicted at the More Reliable CCSD(T)/cc-pV5Z(-PP), CCSD(T)/cc-pwCV5Z(-PP), and the CCSD(T)/CBS Levels

	basis set	SiH	SiF	SiCl	SiBr	SiI
$E(^4\Sigma^-)$	cc-pVTZ	−289.48587	−388.63607	−748.64704	−704.67097	−583.81213
	cc-pVQZ	−289.49230	−388.67873	−748.67841	−704.75608	−583.89904
	cc-pV5Z	−289.49413	−388.69288	−748.68895	−704.83799	−583.95724
	cc-pwCVQZ	−289.49316	−388.68372	−748.68339	−705.16230	−584.34306
	cc-pwCV5Z	−289.49439	−388.69489	−748.69119	−705.19457	−584.37695
	CBS	−289.49529	−388.70379	−748.69840	−705.22786	−584.41209
$E(^2\Pi)$	cc-pVTZ	−289.54652	−388.76636	−748.75728	−704.77406	−583.90303
	cc-pVQZ	−289.55367	−388.80950	−748.78958	−704.86037	−583.99146
	cc-pV5Z	−289.55587	−388.82411	−748.80053	−704.94290	−584.05041
	cc-pwCVQZ	−289.55478	−388.81472	−748.79468	−705.26689	−584.43561
	cc-pwCV5Z	−289.55622	−388.82621	−748.80283	−705.29960	−584.47005
	CBS	−289.55733	−388.83544	−748.81041	−705.33335	−584.50575
$\Delta E(a^4\Sigma^- - X^2\Pi)$	cc-pV5Z	1.680	3.571	3.036	2.855	2.535
	cc-pwCV5Z	1.683	3.574	3.038	2.858	2.533
	CBS	1.688	3.582	3.048	2.871	2.549
	CBS+Δgap$_{(SO)}$	1.696	3.591	3.060	2.888	2.564
	basis set	GeH	GeF	GeCl	GeBr	GeI
$E(^4\Sigma^-)$	cc-pVTZ	−294.02367	−393.14305	−753.17413	−709.20375	−588.35109
	cc-pVQZ	−294.09287	−393.24493	−753.26672	−709.35085	−588.50091
	cc-pV5Z	−294.17679	−393.34019	−753.35879	−709.51468	−588.64111
	cc-pwCVQZ	−294.45613	−393.61067	−753.63400	−710.1203	−588.30874
	cc-pwCV5Z	−294.47921	−393.64357	−753.66334	−710.1741	−589.36421
	CBS	−294.50330	−393.67551	−753.69360	−710.2304	−589.42225
$E(^2\Pi)$	cc-pVTZ	−294.09244	−393.29282	−753.29980	−709.31951	−588.45109
	cc-pVQZ	−294.16303	−393.39812	−753.39532	−709.46950	−588.60378
	cc-pV5Z	−294.24748	−393.49468	−753.48835	−709.63441	−588.74518
	cc-pwCVQZ	−294.52802	−393.76740	−753.76499	−710.24085	−589.41271
	cc-pwCV5Z	−294.55133	−393.80088	−753.79499	−710.29542	−589.46900
	CBS	−294.57565	−393.83341	−753.82575	−710.35235	−589.52789
$\Delta E(a^4\Sigma^- - X^2\Pi)$	cc-pV5Z	1.924	4.204	3.526	3.258	2.832
	cc-pwCV5Z	1.962	4.281	3.582	3.300	2.852
	CBS	1.969	4.297	3.596	3.320	2.874
	CBS+Δgap$_{(SO)}$	2.019	4.343	3.641	3.372	2.875
	basis set	SnH	SnF	SnCl	SnBr	SnI
$E(^4\Sigma^-)$	cc-pVTZ	−213.99378	−313.12164	−673.15395	−629.18322	−508.32891
	cc-pVQZ	−214.05309	−313.21378	−673.23619	−629.31950	−508.46813
	cc-pV5Z	−214.10963	−313.28114	−673.30024	−629.45583	−508.58095
	cc-pwCVQZ	−214.42182	−313.58508	−673.60845	−630.09452	−509.28173
	cc-pwCV5Z	−214.44536	−313.61862	−673.63837	−630.14892	−509.33773
	CBS	−214.46995	−313.65123	−673.66907	−630.20571	−509.39635
$E(^2\Pi)$	cc-pVTZ	−214.05967	−313.25586	−673.27103	−629.29252	−508.42544
	cc-pVQZ	−214.12101	−313.35298	−673.35738	−629.43269	−508.56828
	cc-pV5Z	−214.17815	−313.42237	−673.42295	−629.57049	−508.68258
	cc-pwCVQZ	−214.49239	−313.72961	−673.73370	−630.21109	−509.38411
	cc-pwCV5Z	−214.51617	−313.76386	−673.76421	−630.26620	−509.44095
	CBS	−214.54100	−313.79715	−673.79554	−630.32371	−509.50044
$\Delta E(a^4\Sigma^- - X^2\Pi)$	cc-pV5Z	1.865	3.843	3.339	3.120	2.765
	cc-pwCV5Z	1.927	3.952	3.424	3.191	2.809
	CBS	1.933	3.971	3.441	3.211	2.832
	CBS+Δgap$_{(SO)}$	2.051	4.076	3.526	3.311	2.897
	basis set	PbH	PbF	PbCl	PbBr	PbI
$E(^4\Sigma^-)$	cc-pVTZ	−192.49143			−607.68541	−486.83658
	cc-pVQZ	−192.57477		−651.75421	−607.84404	−486.99840
	cc-pV5Z	−192.64535	−291.78773[a]	−651.83192	−608.00013	−487.12489
	cc-pwCVQZ	−192.85472	−291.99056[b]	−652.03261[b]	−608.52439[b]	−487.71697[b]
	cc-pwCV5Z	−192.87481	−292.01945[b]	−652.05872[b]	−608.57511[b]	−487.76941[b]
	CBS	−192.89576	−292.04593[b]	−652.08542[b]	−608.62799[b]	−487.82424[b]
$E(^2\Pi)$	cc-pVTZ	−192.57017	−291.75922	−651.78208	−607.80528	−486.93988
	cc-pVQZ	−192.65535	−291.88014	−651.89201	−607.96875	−487.10612

Table 1. continued

	basis set	PbH	PbF	PbCl	PbBr	PbI
	cc-pV5Z	−192.72650	−291.96422	−651.97214	−608.12141	−487.23519
	cc-pwCVQZ	−192.93602	−292.16664	−652.17803	−608.65710	−487.83177
	cc-pwCV5Z	−192.95624	−292.19758	−652.20496	−608.70863	−487.88504
	CBS	−192.97733	−292.22723	−652.23250	−608.76237	−487.94075
$\Delta E(a^4\Sigma^- - X^2\Pi)$	cc-pV5Z	2.208	4.803[a]	3.816	3.459	3.000
	cc-pwCV5Z	2.216	4.847[b]	3.980[b]	3.633[b]	3.147[b]
	CBS	2.219	4.933[b]	4.002[b]	3.657[b]	3.171[b]
	CBS+Δgap$_{(SO)}$	2.460	4.9[b]	4.107[b]	3.793[b]	3.209[b]

[a]For the quartet PbF state that is not a stationary point, only single point energy is computed at the doublet equilibrium geometry. [b]For the quartet PbX (X = F, Cl, Br, I) states, since the cc-pwCVnZ (n = Q, 5) potential curves are dissociative, the energies are evaluated for the CBS geometries of the doublet $X^2\Pi$ states.
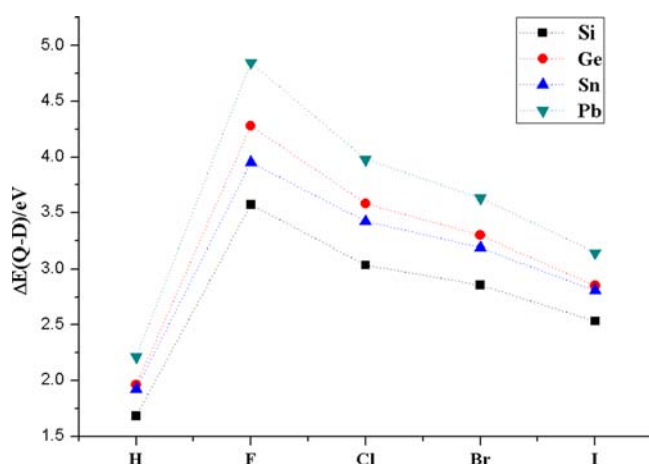

Figure 1. Quartet-doublet splittings ΔE(Q-D) (in eV) predicted by the CCSD(T)/cc-pwCV5Z(-PP) method.

and PbBr, respectively, and this is consistent with the trend of the ΔE(Q-D) values SiBr < SnBr < GeBr < PbBr (Figure 1). Furthermore, these two molecular orbitals are mainly constructed by the valence s and p$_\pi$ atomic orbitals of group 14 elements, and the same trend is found for the $\Delta E(^3P_g - {}^5S_u)$ atomic energy differences, which are 4.13 (Si), 5.20 (Ge), and 4.91 (Sn) eV.[56] This unusual Ge−Sn order may also be

correlated with the nonsystematic order of Pauling electronegativities: 2.01 for Ge and 1.96 for Sn.

We observe that with the cc-pwCV5Z(-PP) basis sets, the quartet ($^4\Sigma^-$) state for PbX (X = F, Cl, Br, I) is not a valence bound stationary point but essentially dissociative. Therefore, in Table 1 we report the quartet single point energies at the analogous doublet equilibrium geometries.

3.2. Doublet and Quartet Structures. Table 2 reports the bond distances for both doublet and quartet structures. The experimental and some previous theoretical bond distances for the ground state E-X compounds are also listed in Table 2 for comparison, and we can see the reasonable agreement with our theoretical values,[57−65] and the previous theoretical results.[23,66] For example, both the CCSD(T)/cc-pwCV5Z method and the CBS limit predict the Si−H distance in the $^2\Pi$ state to be 1.522 Å, which is close to the experimental value of 1.520 Å for the ground state.[57] For PbH, our theoretical bond distance is 1.840 Å at the CCSD(T)/cc-pwCV5Z(-PP) level, or 1.841 Å at the CBS limit level. Agreement with the experimental value 1.839 Å is also satisfactory. For PbF, our theoretical bond distance 2.044 Å at the CCSD(T)/cc-pwCV5Z(-PP) level (or 2.045 Å at the CBS level) falls between the two experimental values, 2.06 Å and 2.03 Å.[58] The previous theoretical bond distances[23] for the $X^2\Pi$ states of SiH, SiF, and SiCl species at the CCSD(T)/aug-cc-pV(n+d)Z (n = T, Q, 5) level of theory are also close to the present results (Table 2).
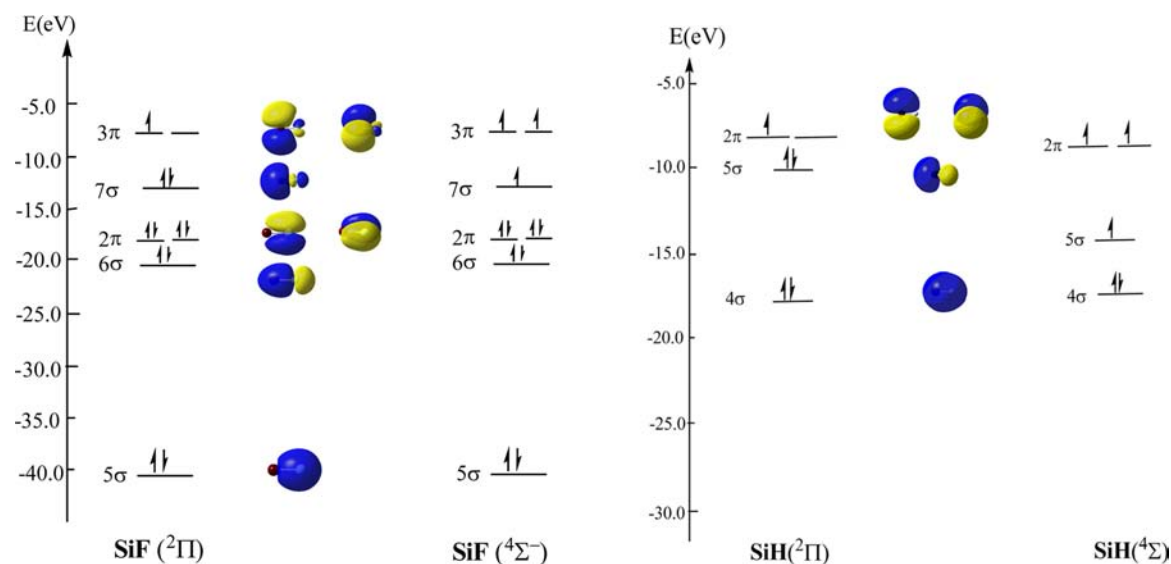

Figure 2. Occupied frontier orbitals for the SiF and SiH electronic states.

Table 2. E-H and E-X Bond Distances (R_e in Å) for the Doublet (D) and Quartet (Q) Structures (E = Si, Ge, Sn, Pb, X = F, Cl, Br, I) Predicted by the CCSD(T) Method with Different Basis Sets

			H	F	Cl	Br	I
Si	$^2\Pi$	cc-pVTZ	1.528	1.620	2.084	2.239	2.458
		cc-pVQZ	1.524	1.611	2.073	2.225	2.446
		cc-pV5Z	1.522	1.607	2.066	2.221	2.439
		cc-pwCVQZ	1.522	1.606	2.066	2.223	2.441
		cc-pwCV5Z	1.522	1.606	2.065	2.221	2.439
		CBS	1.522	1.606	2.063	2.220	2.437
		aug-cc-pV(T+d)Z[b]	1.525	1.615	2.079		
		aug-cc-pV(Q+d)Z[b]	1.523	1.609	2.069		
		aug-cc-pV(5+d)Z[b]	1.522	1.607	2.066		
		DK-Coupled-Cluster[c]	1.522				
		exp.	1.520[57]	1.6011[59] 1.6010[60]	2.061[61] 2.057[59]		
	$^4\Sigma^-$	cc-pVTZ	1.501	1.626	2.082	2.246	2.481
		cc-pVQZ	1.497	1.615	2.066	2.227	2.461
		cc-pV5Z	1.496	1.611	2.059	2.222	2.452
		cc-pwCVQZ	1.495	1.610	2.060	2.226	2.457
		cc-pwCV5Z	1.495	1.610	2.057	2.223	2.453
		CBS	1.496	1.610	2.055	2.219	2.448
Ge	$^2\Pi$	cc-pVTZ	1.584	1.746	2.172	2.318	2.528
		cc-pVQZ	1.572	1.741	2.169	2.310	2.518
		cc-pV5Z	1.574	1.743	2.164	2.306	2.510
		cc-pwCVQZ	1.583	1.742	2.165	2.310	2.514
		cc-pwCV5Z	1.584	1.742	2.163	2.308	2.512
		CBS	1.584	1.743	2.162	2.306	2.510
		CCSD(T,full)/cc-pVTZ[c]		1.744			
		DK-coupled-cluster[c]	1.587				
		exp.	1.588[64]	1.7462(($^2\Pi_{1/2}$), 1.7443($^2\Pi_{3/2}$)[34] 1.7495[63]			
	$^4\Sigma^-$	cc-pVTZ	1.553	1.748	2.186	2.364	2.622
		cc-pVQZ	1.542	1.740	2.178	2.349	2.600
		cc-pV5Z	1.544	1.740	2.171	2.343	2.584
		cc-pwCVQZ	1.557	1.741	2.179	2.363	2.619
		cc-pwCV5Z	1.558	1.741	2.174	2.356	2.609
		CBS	1.559	1.740	2.170	2.350	2.599
Sn	$^2\Pi$	cc-pVTZ	1.774	1.953	2.376	2.517	2.724
		cc-pVQZ	1.759	1.940	2.361	2.498	2.705
		cc-pV5Z	1.747	1.937	2.358	2.491	2.695
		cc-pwCVQZ	1.766	1.935	2.360	2.499	2.702
		cc-pwCV5Z	1.766	1.936	2.357	2.497	2.700
		CBS	1.767	1.937	2.355	2.495	2.697
		DK-coupled-cluster[c]	1.771				
		exp.	1.78[62,59]	1.942[65]	2.361($^2\Pi_{1/2}$), 2.356($^2\Pi_{3/2}$)[58]		
	$^4\Sigma^-$	cc-pVTZ	1.738	1.945	2.374	2.541	2.793
		cc-pVQZ	1.727	1.928	2.354	2.515	2.767
		cc-pV5Z	1.710	1.922	2.351	2.515	2.751
		cc-pwCVQZ	1.738	1.923	2.359	2.533	2.795
		cc-pwCV5Z	1.739	1.922	2.354	2.526	2.783
		CBS	1.740	1.921	2.349	2.520	2.772
Pb	$^2\Pi$	cc-pVTZ	1.849	2.060	2.473	2.608	2.806
		cc-pVQZ	1.823	2.044	2.455	2.587	2.786
		cc-pV5Z	1.814	2.043	2.435	2.585	2.775
		cc-pwCVQZ	1.840	2.042	2.458	2.592	2.786
		cc-pwCV5Z	1.840	2.044	2.455	2.589	2.783
		CBS	1.841	2.045	2.453	2.586	2.780
		exp.	1.839[77]	2.06($^2\Pi_{1/2}$)[58] 2.03($^2\Pi_{3/2}$)[58]			
	$^4\Sigma^-$	cc-pVTZ	1.898	a		3.757	3.481
		cc-pVQZ	1.854	a	3.335	3.275	3.292
		cc-pV5Z	1.845	a	3.102	3.105	3.191
		cc-pwCVQZ	1.919	a	a	a	a
		cc-pwCV5Z	1.920	a	a	a	a
		CBS	1.922	a	a	a	a

Table 2. continued

[a]The quartet PbF is dissociative. [b]Theoretical values from ref 23. [c]Theoretical values from ref 66.
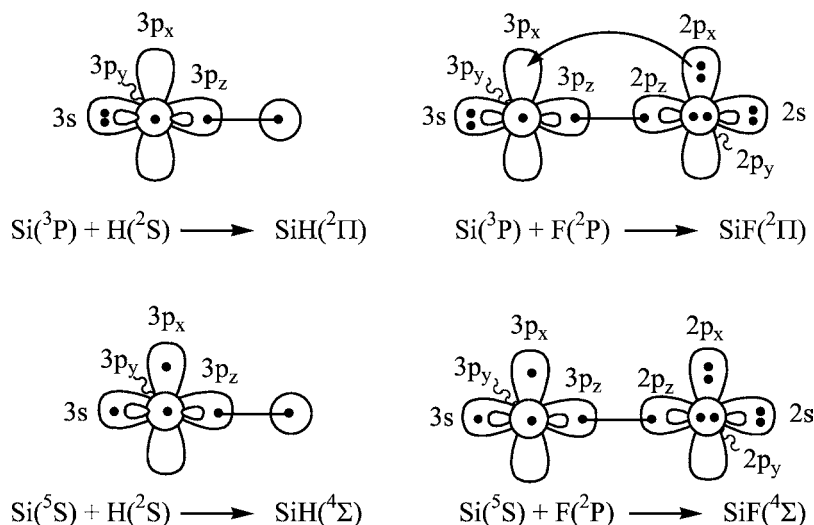

Figure 3. Valence-bond-Lewis diagrams for the SiH and SiF electronic states.

Table 3. Dissociation Energies (D_e, in eV) for the Doublet Ground States ($X^2\Pi$) at the CCSD(T)/cc-pV5Z, CCSD(T)/cc-pwCV5Z, and CCSD(T)/CBS Levels of Theory and Those with the Spin-Orbit Coupling Effect Corrections, D_e(CBS) + ΔD_{SO}

		H	F	Cl	Br	I
Si	D_e(cc-pV5Z)	3.18	6.11	4.40	3.89	3.32
	D_e(cc-pwCV5Z)	3.19	6.13	4.41	3.86	3.28
	D_e(CBS)	3.20	6.17	4.46	3.92	3.33
	D_e(CBS)+ΔD_{SO}	**3.19**	**6.15**	**4.43**	**3.80**	**3.10**
	exp. (D_e)	3.06 ± 0.06^a	5.62^b			
	exp. (D_o)	3.04 ± 0.02^c $<3.06^b$	5.974 ± 0.176^c 5.976^d	4.319 ± 0.065^c 4.29 ± 0.09^e	3.712 ± 0.087^c 3.67 ± 0.09^e	2.520 ± 0.087^c 3.0 ± 0.1^f
Ge	D_e(cc-pV5Z)	2.99	5.35	4.11	3.70	3.22
	D_e(cc-pwCV5Z)	2.94	5.32	4.08	3.64	3.14
	D_e(CBS)	2.95	5.37	4.13	3.69	3.19
	D_e(CBS)+ΔD_{SO}	**2.89**	**5.31**	**4.07**	**3.51**	**2.90**
	exp. (D_e)	3.1 ± 0.2^g				
	exp. (D_o)	2.728 ± 0.050^c $>2.33(2.73)^h$	5.421 ± 0.135^c 5.2^i	4.050 ± 0.099^c 4.0 ± 0.1^j	3.596 ± 0.083^c 3.5^b	2.778 ± 0.259^c
Sn	D_e(cc-pV5Z)	2.76	5.03	3.98	3.61	3.17
	D_e(cc-pwCV5Z)	2.69	5.02	3.95	3.55	3.08
	D_e(CBS)	2.70	5.08	4.01	3.60	3.14
	D_e(CBS)+ΔD_{SO}	**2.53**	**4.90**	**3.84**	**3.30**	**2.73**
	exp. (D_e)					
	exp. (D_o)	2.736 ± 0.176^c $<2.73^k$	4.933 ± 0.083^c 4.90^l	3.628 ± 0.083^c	3.493 ± 0.135^c	2.436 ± 0.031^c
Pb	D_e(cc-pV5Z)	2.59	4.69	3.83	3.51	3.11
	D_e(cc-pwCV5Z)	2.51	4.67	3.79	3.44	3.01
	D_e(CBS)	2.53	4.73	3.85	3.49	3.07
	D_e(CBS)+ΔD_{SO}	**1.84**	**4.00**	**3.12**	**2.65**	**2.10**
	exp. (D_e)	$<1.686^b$	$3.69(9)^k$			
	exp. (D_o)	$<1.627^c$	3.679 ± 0.135^c 3.60^m	3.120 ± 0.518^c 3.101 ± 0.520^n	2.576 ± 0.151^c 2.576 ± 0.152^n	2.011 ± 0.394^c 1.997 ± 0.087^n

[a]Reference 67. [b]Reference 59. [c]Reference 68. [d]Reference 70. [e]Reference 71. [f]Reference 61. [g]Reference 72. [h]Reference 64. [i]Reference 73. [j]Reference 74. [k]Reference 58. [l]Reference 65. [m]Reference 76. [n]Reference 75.

Table 2 shows that, for the hydrides SiH, GeH, and SnH, the E-H bond distances at quartet states are *shorter* than those in the doublet states by ~0.03 Å. However, for most halide compounds E-X (E = Si, Ge, Sn, Pb; X = F, Cl, Br, I) the E-X distances in the quartet states are *longer* or *slightly shorter* than

those in the doublet states (Table 2). This different trend for hydrides and halides may be explained with the orbital diagrams (Figure 3). Taking SiH versus SiF as an example, we can see that the doublet SiH ($^2\Pi$) has a σ bond, while the quartet SiH ($^4\Sigma^-$)state has one unpaired electron on the Si $3p_x$ orbital,

which can be used to form a π bonding, increasing the Si–H bond order and shortening the Si–H distance. On the contrary, the doublet SiF ($^2\Pi$) state has a σ bond and a π bond (from F $2p_x$ to Si $3p_x$), while in the quartet SiF ($^4\Sigma^-$) case, the unpaired electron on the Si $3p_x$ orbital can only form a π antibonding orbital because of the Pauli principle. Thus the $^4\Sigma^-$ state for SiF (and other E-X species) will have somewhat smaller bond orders, lengthening the E-X distances.

In Table 2, we can observe that the $^4\Sigma^-$ states for all haloplumbynes PbX display a different behavior from the other halides. The CCSD(T)/cc-pwCV5Z method predicts the PbX (X = F, Cl, Br, I) molecules to be dissociative. In examining the electronic structures of the PbX (X = F, Cl, Br, I) compounds, a different quartet ($^4\Pi$) state was found to lie in energy close to the $^4\Sigma^-$ state. This is because the $(n-1)\pi$ and $n\sigma$ orbitals have very similar orbital energies in the haloplumbynes PbX, and the $^4\Pi$ state has the $n\sigma^2(n-1)\pi^3n\pi^2$ electron configuration, instead of the $(n-1)\pi^4n\sigma\ n\pi^2$ configuration for the $^4\Sigma^-$ state. The $^4\Pi$ states should have slightly shorter Pb-X distances than those of the analogous $^4\Sigma^-$ states, because the σ bond is usually stronger than the π bond. However, for the other EX (E = Si, Ge, Sn) molecules the $^4\Pi$ states have much higher energies than the $^4\Sigma^-$ states with the $(n-1)\pi^4n\sigma n\pi^2$ electron configuration.

3.3. Dissociation Energies and Dipole Moments. The dissociation energies are given in Table 3 for all the EX (E = Si, Ge, Sn, Pb; X = H, F, Cl, Br, I) diatomics with respect to the E atom in its ground ^3P_g state and the X atom in the ^2P_u ground state. The trend of the dissociation energies for the E-X (X = F, Cl, Br, I) $^2\Pi$ ground state structures is shown in Figure 4. The
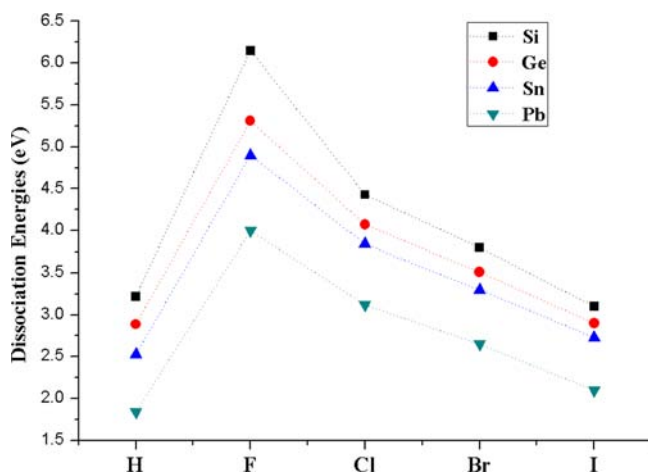
Figure 4. Dissociation Energies (in eV) for the doublet states ($X^2\Pi$) at the CCSD(T)/CBS level with SOC corrections.

hydrides E-H in their $^2\Pi$ states have much smaller dissociation energies than the halides E-X. This may be explained with the Lewis diagram (Figure 3). The halides in their $^2\Pi$ states have an extra π bond, which is absent in the hydrides, and this picture suggests stronger bonds for the halides and thus larger dissociation energies than for the hydrides. With respect to the halides of the same group 14 element E (E = Si–Pb), the dissociation energies decrease as we move from F to Cl, Br, and I. This is because the π-bonding weakens as the E-X distance increases.

Our theoretical dissociation energies are compared with the available experimental results in Table 3.[58,59,61,64,65,67−76] The experimental dissociation energy for ground state SiH was

reported as 3.06 ± 0.06 eV,[67] while our CCSD(T)/CBS result is very close, 3.20 eV. For the halosilylynes (SiF, SiCl, SiBr), the present theoretical results are also comparable to experiment. The latest experimental dissociation energies for SiCl and SiBr are 4.29 ± 0.09 eV and 3.67 ± 0.09 eV,[71] respectively. Our theoretical results (without spin−orbit coupling corrections) of 4.46 eV for SiCl and 3.92 eV for SiBr are somewhat higher than the experimental values. Our theoretical D_e for SiI (3.33 eV) is 0.3 eV too high, compared with the experimental result of 3.0 ± 0.1 eV. However, for Sn and Pb compounds, our theoretical results are even higher. The deviations for the molecules containing heavy atoms may arise from spin−orbit coupling effects. Actually, in a previous study by Balasubramanian,[69] the theoretical dissociation energies for SnCl was given to be as low as 3.34 eV ($X^2\Pi_{1/2}$) or 2.99 eV ($X^2\Pi_{3/2}$)[69] after the spin−orbit coupling effects is considered. Thus, we will further discuss the spin−orbit coupling effects in Section 3.5. It can be seen from Table 3 that the predicted dissociation energies at different theoretical levels agree well with each other.

Theoretical dipole moments for EH (E = Si−Pb) and GeX (X = F, Cl, Br) were reported earlier.[77−81] The only experimental dipole moment available is for GeH with the value $\mu = 1.24 \pm 0.1$ D, but it has been strongly questioned by a previous theoretical study.[77] Like the previous theoretical work, the present theoretical dipole moment for GeH (0.083 D) molecule also significantly disagrees with the experimental value. For the doublet state of SiH, the Mavridis theoretical dipole moment $\mu = 0.124$ D[19] estimated by the FCI method at the MRD-CI results is close to the present result of 0.138 D. For SnF, the previous dipole moment 2.620 D[82] predicted by the SOCI and MRSDCI methods is also close to the present value of 2.614 D.

In the present paper, the dipole moments for all the molecules at the CCSD(T)/cc-pV5Z level are evaluated as expectation values with the CFOUR program (Table 4). For

Table 4. Dipole Moments (in Debye) for the Optimized $X^2\Pi$ and $^4\Sigma^-$ Structures Predicted by CCSD(T)/cc-pV5Z

		H	F	Cl	Br	I
Si	$^2\Pi$	0.138	0.894	0.833	0.782	0.641
	$^4\Sigma^-$	0.023	1.277	0.841	0.488	0.013
Ge	$^2\Pi$	0.083[a]	1.837	1.680	1.540	1.311
	$^4\Sigma^-$	0.172	1.645	0.715	0.200	0.401
Sn	$^2\Pi$	0.368	2.614	2.562	2.405	2.149
	$^4\Sigma^-$	0.049	2.226	1.305	0.742	0.049
Pb	$^2\Pi$	0.878	3.518	3.585	3.412	3.137
	$^4\Sigma^-$	0.255		0.209	0.344	0.582

[a]The experimental dipole moment for GeH is reported to be 1.24 ± 0.1 debye.[77]

the ground $X^2\Pi$ states, the dipole moments in each column increase from silicon toward lead except for SiH. In each row except lead (where PbCl has the largest dipole moment), the dipole moment values decrease from fluorine to iodine.

3.4. Harmonic Vibrational Frequencies. Our theoretical harmonic vibrational frequencies evaluated at the CCSD(T)/cc-pV5Z level for the E-X species are reported in Table 5. Most of these are close to the available experimental values.[34,58−63,65,79−84] For example, the experimental vibrational frequencies for SiF were reported to be 857.6 cm^{-1} for the ground $X^2\Pi$ state and 863 cm^{-1} for the $a^4\Sigma^-$ state, and these

Table 5. Harmonic Vibrational Frequencies (in cm^{-1}) for the X$^2\Pi$ and a$^4\Sigma^-$ Electronic States Predicted at the CCSD(T)/cc-pV5Z Level of Theory

		H		F		Cl		Br		I	
		theo.	exp.	theo.	exp.	theo.	exp.	theo.	exp.	theo.	exp.
Si	$^2\Pi$	2109	2041.80[59]	858	857.6[61,59]	537	535.6[61,59,84]	428	425.4[61]	368	363.8[61]
	$^4\Sigma^-$	2065		864	863[59]	536		408		325	
Ge	$^2\Pi$	1930	1833.77[59]	673	666[34,81] 670 ± 80[83]	409	404[79]	300	295[80]	249	
	$^4\Sigma^-$	1844		655		361		228		166	
Sn	$^2\Pi$	1739	1715[62]	591	577.6[65,82]	356	357($^2\Pi_{1/2}$)[58] 364($^2\Pi_{3/2}$)[58]	254		204	
	$^4\Sigma^-$	1647	1521[62]	588		319		203		143	
Pb	$^2\Pi$	1611	1564.1[63,57]	526	503($^2\Pi_{1/2}$)[58] 520($^2\Pi_{3/2}$)[58]	332	304($^2\Pi_{1/2}$)[58] 322($^2\Pi_{3/2}$)[58]	220		174	161($^2\Pi_{1/2}$)[59] 169($^2\Pi_{3/2}$)[59]
	$^4\Sigma^-$	1015				35		38		46	

Table 6. Energy Differences (in eV) Due to Spin-Orbit Coupling (SOC) Effects for the Ge, Sn, and Pb Atoms (^{3}P, ^{1}D, and ^{1}S States) and the Br and I Atoms (^{2}P State) Using the CASSCF/cc-pwCVTZ(PP) Method[a]

		Ge			Sn			Pb		
	J	$E_{SOC}-E_o$	E_{theo}	E_{exp}	$E_{SOC}-E_o$	E_{theo}	E_{exp}	$E_{SOC}-E_o$	E_{theo}	E_{exp}
^{3}P$_J$	0	−0.12	0.00	0.00	−0.32	0.00	0.00	−1.24	0.00	0.00
	1	−0.05	0.06	0.07	−0.13	0.19	0.21	−0.41	0.83	0.97
	2	+0.05	0.16	0.17	+0.09	0.41	0.43	+0.04	1.27	1.32
^{1}D$_J$	2	+1.05	1.18	0.88	+0.99	1.31	1.07	+1.30	2.54	2.66
^{1}S$_J$	0	+1.99	2.10	2.03	+1.87	2.19	2.13	+2.34	3.57	3.65

		Br			I		
	J	$E_{SOC}-E_o$	E_{theo}	E_{exp}	$E_{SOC}-E_o$	E_{theo}	E_{exp}
^{2}P$_J$	3/2	−0.15	0.00	0.00	−0.30	0.00	0.00
	1/2	+0.29	0.44	0.46	+0.60	0.90	0.94

[a] The corresponding relative energies including spin-orbit coupling effects (E_{theo}, in eV) are reported. The experimental results (E_{exp}, in eV) are also given for comparison. E_o is the ground state energy without SOC effects.

Table 7. Spin-Orbit Coupling Corrections (in eV) for the Doublet E-X Species at the Dissociation Limits (R = 100 Å) ΔE_{super}, Those at the CCSD(T)/CBS Optimized Distances ΔE, and the SOC Corrections for Dissociation Energy $\Delta D_{SO} = \Delta E - \Delta E_{super}$ (in eV) and the SOC Corrections for Quartet-Doublet Gaps $\Delta gap_{(SO)} = [\Delta E(a^4\Sigma^-) - \Delta E(X^2\Pi)]$

		H	F	Cl	Br	I
Si	$\Delta E_{super}(X^2\Pi)$	−0.013	−0.028	−0.043	−0.142	−0.295
	$\Delta E(X^2\Pi)$	−0.008	−0.009	−0.012	−0.025	−0.068
	ΔD_{SO}	**−0.005**	**−0.019**	**−0.031**	**−0.117**	**−0.227**
	$\Delta E(a^4\Sigma^-)$	0.000	0.000	0.000	−0.008	−0.053
	$\Delta gap_{(SO)}$	**+0.008**	**+0.009**	**+0.012**	**+0.017**	**+0.015**
Ge	$\Delta E_{super}(X^2\Pi)$	−0.110	−0.108	−0.107	−0.250	−0.403
	$\Delta E(X^2\Pi)$	−0.053	−0.049	−0.049	−0.072	−0.113
	ΔD_{SO}	**-0.057**	**-0.059**	**-0.058**	**-0.177**	**-0.290**
	$\Delta E(a^4\Sigma^-)$	−0.003	−0.003	−0.004	−0.020	−0.112
	$\Delta gap_{(SO)}$	**+0.050**	**+0.046**	**+0.045**	**+0.052**	**+0.001**
Sn	$\Delta E_{super}(X^2\Pi)$	−0.303	−0.303	−0.301	−0.444	−0.597
	$\Delta E(X^2\Pi)$	−0.136	−0.127	−0.128	−0.147	−0.183
	ΔD_{SO}	**−0.167**	**−0.170**	**−0.173**	**−0.296**	**−0.414**
	$\Delta E(a^4\Sigma^-)$	−0.018	−0.022	−0.043	−0.047	−0.118
	$\Delta gap_{(SO)}$	**+0.118**	**+0.105**	**+0.085**	**+0.100**	**+0.065**
Pb	$\Delta E_{super}(X^2\Pi)$	−1.206	−1.206	−1.206	−1.347	−1.449
	$\Delta E(X^2\Pi)$	−0.515	−0.476	−0.478	−0.504	−0.535
	ΔD_{SO}	**−0.691**	**−0.730**	**−0.731**	**−0.843**	**−0.965**
	$\Delta E(a^4\Sigma^-)$	−0.274	−0.412[a]	−0.373[a]	−0.368[a]	−0.497[a]
	$\Delta gap_{(SO)}$	**+0.241**	**+0.064[a]**	**+0.105[a]**	**+0.136[a]**	**+0.038[a]**

[a] For PbX (X = F, Cl, Br, I), the corrections for the a$^4\Sigma^-$ states are evaluated at the CCSD(T)/CBS geometries of the doublet X$^2\Pi$ states.

results are nearly equal to our theoretical values of 858 cm^{-1} and 864 cm^{-1}, respectively. However, for the EH (E = Si−Pb) molecules, the predicted harmonic vibrational frequencies are larger than the available experimental values.

3.5. Spin−Orbit Coupling Effects. For the heavy elements, such as Br, I, Sn, and Pb, the spin−orbit coupling effects may be significant for the predicted energies.[85,86] The spin−orbital coupling (SOC) effects for the ground $X^2\Pi$ states are evaluated with the MOLPRO program package.[87] The CASSCF method is used, because only the CASSCF wave functions can be used for the full Breit-Pauli spin−orbit coupling operator in the MOLPRO program.[88] Since all the orbitals, including the valence orbitals and the core orbitals, should be considered, the core−valence correlation consistent basis sets are chosen. For the F, Cl, and Si atoms the cc-pwCVTZ basis sets are used.[48] For the heavy atoms the cc-pwCVTZ-PP pseudopotentials including two-component ECPs are used.[53] All the valence shells are included in the CASSCF active space.

Before applying SOC effects to the E-X molecules, we tested this method on the related heavy atoms at the same CASSCF/cc-pwCVTZ(-PP) level of theory. In Table 6, the j level splittings caused by the spin−orbit coupling (SOC) are listed for the ^3P, ^1D, and ^1S states of Ge, Sn, and Pb and those for the ^2P states for Br and I. It can be seen that our theoretical results are in good agreement with the experimental values.[56] Compared with the previous theoretical SOC stabilization energy of −1.23 eV[89] for the Pb atom in its ^3P_J ground state with the all-electron CASPT2/ANO method, our SOC $\Delta E(^3P - {}^3P_0)$ of −1.24 eV is in excellent agreement.

Similar to a previous study of PbO,[89] all states of EH and EX that dissociate to $E(^3P, {}^1D$ or $^1S)$, $X(^2P)$, and $H(^2S)$ were included in the CASSCF state averaged computations. C_2 symmetry is constrained, and the degenerate pairs of the electronic states were averaged. We have predicted the SOC effects on ΔE for these molecules at their CCSD(T)/CBS E-X distances, and we have computed the stabilization energies ΔE_{super} for the supermolecules at $R = 100$ Å (i.e., dissociated atoms). The difference $\Delta D_{SO} = (\Delta E - \Delta E_{super})$ would be the SOC corrections for the dissociation energies of the ground $X^2\Pi$ electronic states (Table 7). As expected, the SOC corrections increase from the molecules with the light atoms to those with the heavy atoms, that is, from H to I and from Si to Pb. For the lightest molecules SiH and SiF, these corrections are the smallest, only 0.005 eV (SiH) and 0.019 eV (SiF). For the heaviest molecule PbI, the SOC correction ΔD_{SO} is as much as ∼1 eV (Table 7).

Our theoretical SOC corrected dissociation energies $D_e + \Delta D_{SO}$ are in much better agreement with the available experimental results (Table 3). For example, the SOC corrected dissociation energy for SiI $(^2\Pi)$ is 3.10 eV, which is within the error bars of the experimental value 3.0 ± 0.1 eV (Table 3). The dissociation energies without the SOC corrections for the heavy molecule PbI $(^2\Pi)$ is 3.07 eV, and the SOC corrected dissociation energy is reduced to 2.10 eV, very close to the experimental value of 2.011 ± 0.394 eV (Table 3).

The quartet-doublet splittings $\Delta E(Q-D)$ for EX molecules were also corrected by the SOC effect at their CCSD(T)/CBS geometries. The corrections $\Delta gap_{(SO)} = [\Delta E(a^4\Sigma^-) - \Delta E(X^2\Pi)]$ are reported in Table 7. Because the quartet $a^4\Sigma^-$ states for PbX (X = F, Cl, Br, I) are dissociative, the analogous corrections for them are computed at the doublet $X^2\Pi$ geometries. Table 7 shows that the SOC corrections for the quartet-doublet splitting are not as significant as those for the dissociation energies, even for the molecules containing heavy atoms. For most of the EX molecules, the SOC corrections for

the quartet-doublet splittings $\Delta E(Q-D)$ are less than 0.1 eV, and the largest is 0.241 eV for PbH, which is still much smaller than the corresponding SOC correction for the dissociation energy (−0.691 eV).

4. CONCLUSIONS

In the present research, the structures of the EX (E = Si−Pb, X = H, F−I) diatomic molecules have been studied using the couple-cluster method CCSD(T) with large basis sets. The equilibrium distances, dipole moments, quartet-doublet energy differences, harmonic vibrational frequencies, and dissociation energies for these species are predicted. The quartet-doublet splittings range from 1.70 eV (SiH) to 3.59 eV (SiF) for the silylynes, from 2.02 eV (GeH) to 4.34 eV (GeF) for the germylynes, from 2.05 eV (SnH) to 4.08 eV (SnF) for the stannylynes, and from 2.46 eV (PbH) to 5.00 eV (PbF) for the plumbylynes. The trend is noticeable: the largest quartet-doublet gaps appear in the fluorides, and decrease toward the iodides. The $X^2\Pi$ dissociation energies follow the same trend. The SiH experimental doublet-quartet energy difference[55] appears to be in serious error. The only other experimentally known $\Delta E(D-Q)$ is that for GeF, and our theoretical prediction agrees well with experiment.[34]

The dissociation energies calculated at CCSD(T)/CBS method level were corrected by the spin−orbit coupling effects (Table 7). When the SOC corrections are added the results from CCSD(T)/CBS method, the trend does not change, decreasing from fluoride to iodide, but the corrections become much larger for the heavier molecules. However, the quartet-doublet splitting changes from the SOC effects are not as large as those for the dissociation energies.

In this study the hydrides and the halodides of group-14 elements were systematically investigated, including not only the experimentally known species but also the unknown yet potentially important species. As Filippou, et al. suggested,[9] three types of mononuclear halosilylyne complexes are conceivable in his studies of the mononuclear chromium complexes. We suggest that other species of group 14 from Ge to Pb also have similar possibilities to form compounds containing multiple metal-X (X = Ge−Pb) bonds.

Generally speaking, these high level theoretical predictions behave in a monotonic manner along the two series: "Si: Ge: Sn: Pb", and "F: Cl: Br: I". However, there are notable exceptions. For example we find for the doublet-quartet energy separations, PbF > GeF > SnF > SiF. Finally, it should be noted that the equilibrium distances of doublet and quartet state structures are very similar for all the halosilylynes, halogermylynes, halostannylidynes. The exception is for the haloplumbylyne quartets, where PbX (X = F, Cl, Br, I) is dissociative.

■ **AUTHOR INFORMATION**

Corresponding Author

*E-mail: Fenghao@mail.xhu.edu.cn (H.F.), qc@uga.edu (H.F.S.).

Notes

The authors declare no competing financial interest.

■ REFERENCES

(1) Bender, C. F.; Schaefer, H. F. *J. Am. Chem. Soc.* **1970**, *92*, 4984.

(2) James, F. C.; Choi, H. K. J.; Ruzsicska, B. P.; Strausz, O. P.; Bell, T. N. The Gas Phase Chemistry of Carbyne. In *Frontiers of Free Radical Chemistry*; Pryor, W. A., Ed.; Academic Press: New York, 1980; pp 139−170.

(3) Ruzsicska, B. P.; Jodhan, A.; Choi, H. K. J.; Strausz, O. P.; Bell, T. N. *J. Am. Chem. Soc.* **1983**, *105*, 2489.

(4) Bogoslavsky, B.; Levy, O.; Kotlyar, A.; Salem, M.; Gelman, F.; Bino, A. *Angew. Chem., Int. Ed.* **2012**, *51*, 90.

(5) Kasdan, A.; Herbst, E.; Lineberger, W. C. *Chem. Phys. Lett.* **1975**, *31*, 78.

(6) Jesinger, R. A.; Squires, R. R. *Int. J. Mass Spectrom.* **1999**, *185−187*, 745.

(7) Lee, V. Ya.; Sekiguchi, A. *Organometallic Compounds of Low-Coordinate Si, Ge, Sn, and Pb: From Phantom Species to Stable Compounds*; Wiley: Chichester, U.K., 2010.

(8) Hashimoto, H.; Fukuda, T.; Tobita, H.; Roy, M.; Sasaki, S. *Angew. Chem., Int. Ed.* **2012**, *51*, 2930.

(9) Filippou, A. C.; Chernov, O.; Schnakenburg, G. *Chem.—Eur. J.* **2011**, *17*, 13574.

(10) Filippou, A. C.; Philippopoulos, A. I.; Portius, P.; Schnakenburg, G. *Organometallics* **2004**, *23*, 4503.

(11) Filppou, A. C.; Barandov, A.; Schnakenburg, G.; Lewall, B.; van Gastel, M.; Marchanka, A. *Angew. Chem., Int. Ed.* **2012**, *51*, 789.

(12) Filippou, A. C.; Stumpf, K. W.; Chernov, O.; Schnakenburg, G. *Organometallics* **2012**, *31*, 748.

(13) Filippou, A. C.; Chernov, O.; Schnakenburg, G. *Angew. Chem., Int. Ed.* **2009**, *48*, 5687.

(14) Jackson, C. V. *Proc. R. Soc. London, Series A* **1930**, *126*, 373.

(15) Kasdan, A.; Herbst, E.; Lineberger, W. C. *J. Chem. Phys.* **1975**, *62*, 541.

(16) Schmitt, J. P. M.; Gressier, P.; Krishnan, M.; Rosny, G. de; Perrin, J. *Chem. Phys.* **1984**, *84*, 281.

(17) Brown, J. M.; Robinson, D. *Mol. Phys.* **1984**, *51*, 883.

(18) Washida, N.; Matsumi, Y.; Hayashi, T.; Ibuki, T.; Hiraya, A.; Shobatake, K. *J. Chem. Phys.* **1985**, *83*, 2769.

(19) Kalemos, A.; Mavridis, A. *J. Chem. Phys.* **2002**, *116*, 6529.

(20) Hildenbrand, D. L.; Lau, K. H.; Sanjurjo, A. *J. Phys. Chem. A* **2003**, *107*, 5448.

(21) Jackson, N. A.; Randall, C. J.; McKendrick, K. G. *J. Phys. Chem. A* **1998**, *102*, 51.

(22) Lein, M.; Krapp, A.; Frenking, G. *J. Am. Chem. Soc.* **2005**, *127*, 6290.

(23) Prascher, B. P.; Lucente-Schultz, R. M.; Wilson, A. K. *Chem. Phys.* **2009**, *359*, 1.

(24) Ricca, A.; Bauschlicher, C. W. *J. Phys. Chem. A* **1998**, *102*, 876.

(25) Feller, D.; Dixon, D. A. *J. Phys. Chem. A* **1999**, *103*, 6413.

(26) Wang, L.; He, Y.-L. *Int. J. Mass Spectrom.* **2008**, *276*, 56.

(27) Ho, P.; Coltrin, M. E.; Binkley, J. S.; Melius, C. F. *J. Phys. Chem.* **1985**, *89*, 4647.

(28) Humbird, D.; Graves, D. B. *J. Chem. Phys.* **2004**, *120*, 2405.

(29) Li, Q.; Li, G.; Xu, W.; Xie, Y.; Schaefer, H. F. *J. Chem. Phys.* **1999**, *111*, 7945.

(30) Hildenbrand, D. L.; Lau, K. H. *Chem. Phys. Lett.* **1996**, *263*, 145.

(31) Antoniotti, P.; Borocci, S.; Bronzolino, N.; Giordani, M.; Grandinetti, F. *J. Phys. Chem. A* **2006**, *110*, 4900.

(32) Wang, J. L.-F.; Margrave, J. L.; Franklin, J. L. *J. Chem. Phys.* **1974**, *60*, 2158.

(33) Harland, P. W.; Cradock, S.; Thynne, J. C. J. *Int. J. Mass Spectrom. Ion Phys.* **1972**, *10*, 169.

(34) Martin, R. W.; Merer, A. J. *Can. J. Phys.* **1973**, *51*, 125.

(35) Bundhun, A.; Ramasami, P.; Gaspar, P. P.; Schaefer, H. F. *Inorg. Chem.* **2012**, *51*, 851.

(36) Zagorevskii, D.; Yuan, Y.; Greenlief, C. M.; Momemer, A. A. *Eur. J. Mass. Spectrom.* **2002**, *8*, 351.

(37) Baklanov, K. I.; Petrov, A. N.; Titov, A. V.; Kozlov, M. G. *Phys. Rev. A* **2010**, *82*, 060501(R).

(38) Alphei, L. D.; Grabow, J.-U.; Petrov, A. N.; Mawhorter, R.; Murphy, B.; Baum, A.; Sears, T. J.; Yang, T. Z.; Rupasinghe, P. M.; McRaven, C. P.; Shafer-Ray, N. E. *Phys. Rev. A* **2011**, *83*, 040501(R).

(39) Mawhorter, R. J.; Murphy, B. S.; Baum, A. L.; Sears, T. J.; Yang, T.; Rupasinghe, P. M.; McRaven, C. P.; Shafer-Ray, N. E.; Alphei, L. D.; Grabow, J.-U. *Phys. Rev. A* **2011**, *84*, 022508.

(40) Shimizu, T.; Frenking, G. *Theor. Chem. Acc.* **2011**, *130*, 269.

(41) Pandey, K. K.; Lledos, A. *Inorg. Chem.* **2009**, *48*, 2748.

(42) Raghavachari, K.; Trucks, G. W.; Pople, J. A.; Head-Gordon, M. *Chem. Phys. Lett.* **1989**, *157*, 479.

(43) Bartlett, R. J.; Watts, J. D.; Kucharski, S. A.; Noga, J. *Chem. Phys. Lett.* **1990**, *165*, 513.

(44) Bartlett, R. J.; Watts, J. D.; Kucharski, S. A.; Noga, J. *Chem. Phys. Lett.* **1990**, *167*, 609.

(45) CFOUR, a quantum chemical program package , Stanton, J. F.; Gauss, J.; Harding, M. E.; Szalay P. G. with contributions from Auer, A. A.; Bartlett, R. J.; Benedikt, U.; Berger, C.; Bernholdt, D. E.; Bomble, Y. J. et al. and the integral packages MOLECULE (Almlöf J.; Taylor P. R.), PROPS (Taylor P. R.), ABACUS (Helgaker, T.; Jensen, H. J. Aa.; Jöügensen, P.; Olsen, J.), and ECP routines (Mitin, A. V.; van Wüllen, C.), 2010.

(46) Dunning, T. H., Jr. *J. Chem. Phys.* **1989**, *90*, 1007.

(47) Woon, D. E.; Dunning, T. H., Jr. *J. Chem. Phys.* **1993**, *98*, 1358.

(48) Peterson, K. A.; Dunning, T. H., Jr. *J. Chem. Phys.* **2002**, *117*, 10548.

(49) Peterson, K. A. *J. Chem. Phys.* **2003**, *119*, 11099.

(50) Peterson, K. A.; Figgen, D.; Goll, E.; Stoll, H.; Dolg, M. *J. Chem. Phys.* **2003**, *119*, 11113.

(51) Peterson, K. A.; Shepler, B. C.; Figgen, D.; Stoll, H. *J. Phys. Chem. A* **2006**, *110*, 13877.

(52) Metz, B.; Stoll, H.; Dolg, M. *J. Chem. Phys.* **2000**, *113*, 2563.

(53) Peterson, K. A.; Yousaf, K. E. *J. Chem. Phys.* **2010**, *133*, 174116.

(54) Helgaker, T.; Klopper, W.; Koch, H.; Noga, J. *J. Chem. Phys.* **1997**, *106*, 9639.

(55) Park, C. *J. Quant. Spectrosc. Radiat. Transf.* **1979**, *21*, 373.

(56) NIST (1999) Atomic Spectra Database Levels, online: http://physics.nist.gov/ PhysRefData/ASD/levels_form.html.

(57) Betrencourt, M.; Boudjaadar, D.; Chollet, P.; Guelachvili, G.; Morillon-Chapey, M. *J. Chem. Phys.* **1986**, *84*, 4121.

(58) Balasubramanian, K. *Chem. Rev.* **1989**, *89*, 1801.

(59) Huber, K. P.; Herzberg, G. *Constants of diatomic molecules*; Van Nostrand/Reinhold: New York, 1979.

(60) Tanaka, T.; Tamura, M.; Tanaka, K. *J. Mol. Struct.* **1997**, *413*, 153.

(61) Billingsley, J. *J. Mol. Spectrosc.* **1972**, *43*, 128.

(62) Balasubramanian, K.; Pitzer, K. S. *J. Mol. Spectrosc.* **1984**, *103*, 105.

(63) Tanimoto, M.; Saito, S.; Endo, Y.; Hirota, E. *J. Mol. Spectrosc.* **1986**, *116*, 499.

(64) Ruscic, B.; Schwarz, M.; Berkowitz, J. *J. Chem. Phys.* **1990**, *92*, 1865.

(65) Gurvich, L. V.; Veyts, I. V.; Alcock, C. B. *Thermodynamic Properties of Individual Substances*, 4th ed.; Hemisphere: New York, 1991; Vol. 2, Part I.

(66) Hirata, S.; Yanai, T.; de Jong, W. A.; Nakajima, T.; Hirao, K. *J. Chem. Phys.* **2004**, *120*, 3297.

(67) Verma, R. D. *Can. J. Phys.* **1965**, *43*, 2136.

(68) Luo, Y.-R. *Comprehensive Handbook of Chemical Bond Energies*; CRC Press: Boca, Raton, FL, 2007.

(69) Balasubramanian, K. *J. Mol. Spectrosc.* **1988**, *132*, 280.

(70) Fisher, E. R.; Kickel, B. L.; Armentrout, P. B. *J. Phys. Chem.* **1993**, *97*, 10204.

(71) Hildenbrand, D. L.; Lau, K. H.; Sanjurjo, A. *J. Phys. Chem. A* **2003**, *107*, 5448.

(72) Balasubramanian, K.; Li, J. *J. Mol. Spectrosc.* **1988**, *128*, 413.

(73) Martin, R. W.; Merer, A. J. *Can. J. Phys.* **1974**, *52*, 1458.

(74) Hildenbrand, D. L.; Lau, K. H. *Chem. Phys. Lett.* **1996**, *263*, 145.

(75) Drake, L. R.; Simons, J. W.; Oldenborg, R. C. *J. Phys. Chem.* **1995**, *99*, 11350.

(76) Kozlov, M. G.; Fomicher, V. I.; Dimtriev, Yu. Yu.; Labzovsky, L. N.; Titov, A. V. *J. Phys. B: At. Mol. Opt. Phys.* **1987**, *20*, 4939.

(77) Brown, J. M.; Evenson, K. M.; Sears, T. J. *J. Chem. Phys.* **1985**, *83*, 3275.

(78) Chapman, D. A.; Li, J.; Balasubramanian, K.; Lin, S. H. *J. Chem. Phys.* **1988**, *88*, 3826.

(79) Liao, D.-W.; Balasubramanian, K. *Chem. Phys. Lett.* **1993**, *213*, 174.

(80) Liao, D.-W.; Balasubramanian, K. *J. Mol. Spectrosc.* **1993**, *162*, 498.

(81) Liao, D.-W.; Balasubramanian, K. *J. Mol. Spectrosc.* **1994**, *163*, 284.

(82) Dai, D.; Balasubranmanian, K. *Chem. Phys. Lett.* **1994**, *224*, 425.

(83) Negishi, Y.; Kawamata, H.; Hayase, T.; Gomei, M.; Kishi, R.; Hayakawa, F.; Nakajima, A.; Kaya, K. *Chem. Phys. Lett.* **1997**, *269*, 199.

(84) Melen, F.; Doubois, I.; Bredohl, H. *J. Mol. Spectrosc.* **1990**, *139*, 361.

(85) Lindh, B. O. R.; Malmqvist, P.-A.; Veryazov, V.; Widmark, P.-O. *J. Phys. Chem. A* **2004**, *108*, 2851.

(86) Metz, B.; Stoll, H.; Dolg, M. *J. Chem. Phys.* **2000**, *113*, 2563.

(87) MOLPRO is a package of ab initio programs written by Werner, H.-J.; Knowles, P. J.; Knizia, G.; Manby, F. R.; Schütz, M.; Celani, P.; Korona, T.; Lindh, R.; Mitrushenkov, A.; Rauhut, G.; Shamasundar, K. R.; Adler, T. B.; Amos, R. D.; Bernhardsson, A.; Berning, A.; Cooper, D. L.; Deegan, M. J. O.; Dobbyn, A. J.; Eckert, F.; Goll, E.; Hampel, C.; Hesselmann, A.; Hetzer, G.; Hrenar, T.; Jansen, G.; Köppl, C.; Liu, Y.; Lloyd, A. W.; Mata, R. A.; May, A. J.; McNicholas, S. J.; Meyer, W.; Mura, M. E.; Nicklass, A.; O'Neill, D. P.; Palmieri, P.; Peng, D.; Pflüger, K.; Pitzer, R.; Reiher, M.; Shiozaki, T.; Stoll, H.; Stone, A. J.; Tarroni, R.; Thorsteinsson, T.; Wang M..

(88) Berning, A.; Schweizer, M.; Werner, H.-J.; Knowles, P. J.; Palmieri, P. *Mol. Phys.* **2000**, *98*, 1823.

(89) Roos, B. O.; Malmqvist, P.-A. *Adv. Quantum Chem.* **2004**, *47*, 37.